

Hydrophobic polyurethane foams reinforced with microcrystalline cellulose for oil spill clean up

Matheus Vinícius Gregory Zimmermann^{1*} , Eduardo Junca¹ , Marina Kauling de Almeida¹ ,
Lara Vasconcellos Ponsoni¹ , Ademir José Zattera² , Tiago Mari²  and
Ruth Marlene Campomanes Santana³ 

¹ Programa de Pós-graduação em Engenharia e Ciência dos Materiais – PPGCEM, Universidade do Extremo Sul Catarinense – UNESC, Criciúma, SC, Brasil

² Programa de Pós-graduação em Engenharia de Processos e Tecnologias – PGEPROTEC, Universidade de Caxias do Sul – UCS, Caxias do Sul, RS, Brasil

³ Programa de Pós-graduação em Engenharia de Minas, Metalúrgica e de Materiais – PPG3M, Universidade Federal do Rio Grande do Sul – UFRGS, Porto Alegre, RS, Brasil

*e-mail: matheus.vgz@gmail.com

Abstract

Oil spills into water have been an environmental concern since the beginning of large-scale oil extraction. In this study, flexible open-cell polyurethane (PU) foams with added microcrystalline cellulose (MCC) were formulated and chemically modified with organosilane for use as an absorbent system for oil spill cleanup in water. The influence of cellulose concentration on mechanical properties and chemical treatment with organosilane was evaluated. The primary findings indicate that the surface treatment of the solid fraction of the foams was effective, as indicated by the contact angle, increasing the hydrophobicity of the samples. Because of the increased roughness of the PU solid fraction and the cellulose reactivity, the mechanical compressive strength and thickness of the organosilane layer increased with increasing MCC content. However, the higher the MCC content in the composition, the higher was the density, which reduced the sorption capacity of the samples.

Keywords: *polyurethane foams, oil spill cleanup, organosilane, cellulose.*

How to cite: Zimmermann, M. V. G., Junca, E., Almeida, M. K., Ponsoni, L. V. Zattera, A. J., Mari, T., & Santana, R. M. C. (2023). Hydrophobic polyurethane foams reinforced with microcrystalline cellulose for oil spill clean up. *Polímeros: Ciência e Tecnologia*, 33(4), e20230040. <https://doi.org/10.1590/0104-1428.20230054>

1. Introduction

Oil contamination has been an environmental issue since the beginning of large-scale extraction and use of oil. According to the International Tanker Owners Pollution Federation, the total global volume of tanker oil spills in 2022 was approximately 15,000 tons^[1]. Oil spills typically occur during the extraction and transportation processes, causing economic, environmental, and social damage. Oil spilled during maritime extraction kills marine animals, contaminates seafood, produces toxic steam, and its residues can last for decades^[2-5]. Oil spilled into the water spreads immediately. Its volatile components can evaporate and contaminate the air, and it can simultaneously become emulsified in the oil–water, making it difficult to extract and remove^[6].

Some water–oil separation techniques, such as flotation, centrifugation, adsorption, gravimetric separation, electrochemistry, and biodegradation, have been investigated to minimize the impact of oil spills^[4]. The sorption process has been highlighted as a technique for treating industrial effluents and is an effective and economical alternative for remediating areas degraded by oil spills. This process

involves simultaneous absorption, adsorption, and desorption processes. In absorption, the oil is absorbed within the system, and in adsorption, the oil is retained on the surface of the solid part of the sorbent^[7].

For an oleophilic sorbent to be effective, oil must enter the sorbent rapidly, in large quantities, and without causing the sorbent system to rupture or disintegrate. Simultaneously, oil desorption during the sorbent withdrawal from the medium must be low; therefore, the oil must remain within the system until it is removed from the environment^[8]. According to Liu et al.^[9], an ideal sorbent would be a material with a high oil sorption capacity and selectivity to oil but not to water, low density, recyclability, and low environmental aggressiveness. Sorbent materials have a high oil removal capacity, are able to absorb 3–100 times their original mass and have a low environmental impact and cost^[10]. The selectivity for oil (predominantly hydrophobic) of a sorbent for removing apolar materials is the most important property that determines its efficiency in removing apolar materials, especially when oils are in an aquatic environment^[11].

Polyurethane (PU) foams are synthesized via the polymerization reaction between a di or tri isocyanate and a hydroxylated polyol, resulting in a PU chain. PU foams can take various shapes depending on the formation method, such as rigid, semi-rigid, or flexible, with varying densities. Upholstery made of reinforced materials with sorption capacities can benefit from the application of PU^[12]. The viscoelastic properties of foams synthesized with high open-cell concentrations allow for oil sorption and desorption. The development of oleophilic and hydrophobic properties is related to sorption and desorption using reagents like organosilanes for modification during the foam preparation^[13].

Several researchers have used organosilanes as coating agents to produce hydrophobic surfaces. Jianliang et al.^[13] modified the seaweed *Enteromorpha* with organosilanes to maintain its oleophilic properties while becoming hydrophobic, whereas Usman et al.^[14] modified ceramic membranes with organosilanes, both of which intend to use such modifications to remove oil from water. The advantages of using organosilane as a coating include its availability on a large scale, the possibility of being a bifunctional molecule capable of reacting with the surface, and the presence of functional groups that can modify the hydrophobicity of the sample^[15]. The reaction in silanes is based on their bifunctionality (they have two distinct reactive groups); in the presence of water, silane hydrolyzes and forms silanol, which can react with the hydroxyls of the substrate and form covalent and/or secondary bonds on the surface of the substrate^[5,16].

In the production of expanded composites or reinforced foams, another mechanism commonly used to modify the physical and mechanical properties of polymeric foams is the incorporation of fillers. The addition of fillers to polymeric foams can be used to reduce the final cost of the product, increase foam rigidity, or modify specific properties, such as changing surface characteristics, such as roughness, increasing thermal stability, increasing cell nucleation (a greater number of cells and smaller size per unit volume), and facilitating the opening of pores around the cells^[17]. Depending on the type, size, and filler content of the polymeric foams, various cell morphologies can be obtained^[18]. Organic materials derived from plant fibers have recently gained prominence in the field of polymeric composites, owing to their lower abrasiveness and density than those of inorganic materials, being derived from renewable and biodegradable sources, and being easy to obtain (with relatively low cost)^[17]. Among plant fibers, cellulose is the most abundant biopolymer on Earth and is a fundamental component of most plant species. Another important property of cellulose is its ability to be easily chemically modified, making it appealing for use as a reinforcing agent in polymeric composites owing to the combination of chemical affinities that can be obtained^[16,19-21].

Microcrystalline cellulose (MCC) is produced from purified and partially depolymerized cellulose. It can be used as a fine-particle powder or processed with a water-soluble polymer to obtain a colloidal form. MCC can be produced from various cellulose sources; however, cotton and wood are the primary sources used for breeding. The most common applications include binders and fillers in food and medical tablets and as reinforcement reagents for the development of polymer composites. MCC is considered

a potential reinforcement for improving the mechanical properties of the material^[22].

Given the difficulty of cleaning oil spills from water sources around the world, there is a need to develop alternative oil-absorbing options. This study aimed to produce a PU foam reinforced with MCC for use as a sorbent in oil spills and to evaluate the effect of different MCC concentrations on the chemical treatment with organosilane and the physical and mechanical properties of the PU foam.

2. Materials and Methods

2.1 Materials

For the development of PU foams, Voranol WL 4010 polyol and Voranate™ T-80 toluene diisocyanate (TDI, supplied by Dow Brasil Sudeste Industrial Ltda., were used. The amine catalyst (Dabco® 2033 Catalyst) was supplied by Air Products and the organometallic tin octanoate catalyst (Kosmos® 29) was supplied by Evonik Industries. The surfactant, commercially known as Niaux silicone L-595, was supplied by Momentive Performance Materials, Inc. Methylene chloride, a deionizing agent supplied by Brasil Sudeste Industrial Ltd., and deionized water were used.

Sigma-Aldrich S. A supplied MCC, Sigmacell Type 20 grade, particle size approximately 20 μm , code S3504. Triethoxyvinylsilane (TEVS) (supplier code: 175560) and tetraethoxysilane (TEOS) (supplier code: 13190) were used for the hydrophobic coating of PU foams, and were supplied by Sigma-Aldrich.

The following oils were used for the sorption tests: Ipiranga SAE 5W30 oil (lubricating motor oil) with a density of 0.86 $\text{g}\cdot\text{cm}^{-3}$ at 20 °C and a kinematic viscosity of 70 cSt at 40 °C, soybean oil (vegetable oil-cooking oil) with a density of 0.91 $\text{g}\cdot\text{cm}^{-3}$ at 20 °C and a kinematic viscosity of 32 cSt at 40 °C; and kerosene (fuel oil) with a density of 0.78 $\text{g}\cdot\text{cm}^{-3}$ at 20 °C and a kinematic viscosity of 2.2 (max) cSt at 40 °C. Crude oil, supplied by Petrobras, has an °API of 30.2, a density of 0.87 $\text{g}\cdot\text{cm}^{-3}$, and is classified as medium oil.

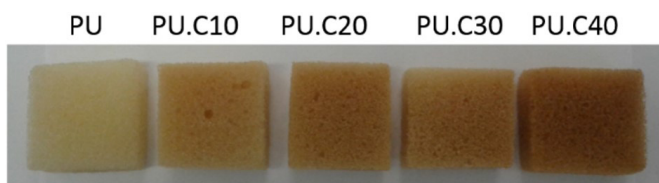
2.2 Methods

Table 1 lists the PU foams formulated with various MCC concentrations expressed in parts per hundred polyols (pphp). In the standard composition of the flexible PU foams, four levels of MCC were used, with a theoretical density of 10 $\text{kg}\cdot\text{m}^{-3}$.

The PU foams were produced via the batch method using a Fisaton 715 propeller mixer at a rotational speed of 2500 rpm. Water, amine, silicone, and various concentrations of MCC were initially added to the polyol and stirred for 80 s. Tin octanoate was then added and mixed for 40–50 s. Thereafter, TDI and methylene chloride were added to the blend while vigorously stirring for approximately 10–15 s, and the mixture was poured into a mold for free expansion to form the foam. The expansion time is approximately 1 min. The foam was cured for 48 h at a constant temperature of 23 °C.

Table 1. Polyurethane foams formulations (pphp).

Reagents	PU 1	PU.C10	PU.C20	PU.C30	PU.C40
Polyol	100	100	100	100	100
Diisocyanate	80	80	80	80	80
Water	6	6	6	6	6
Amine	0.3	0.3	0.3	0.3	0.3
Silicone	3.3	3.3	3.3	3.3	3.3
Octoate	0.5	0.5	0.5	0.5	0.5
Chloride	22	22	22	22	22
MCC	0	10	20	30	40

**Figure 1.** Photographic image of PU foams after organosilane coating.

Hydrophobization of the PU foam was performed using an organosilane-based coating. First, organosilane hydrolysis was performed in a water:alcohol (70:30) solution containing 1% (mass) organosilane TEVS and 1% (mass) TEOS. To stabilize the pH of the solution at 4.5, acetic acid (approximately 10 mL/L of solution) was added dropwise. For 2 h, the resulting solution was stirred. Following that, foam samples (25 mm × 25 mm × 25 mm) were immersed in the solution, and the solution was slowly stirred with a magnetic bar stirrer for 4 h. Later, the foams were removed from the solution, the excess liquid was drained, and the samples were dried at 120 °C for 4 h (with the occurrence of concomitant organosilane curing).

Figure 1 presents photographic images of the foams after the hydrophobic coating, with and without the addition of cellulose, highlighting the change in color of the foams to darker tones as the cellulose content increases. This change in foam color could be attributed to the curing time altering the chemical structure of the cellulose and promoting partial degradation of its constituents.

2.3 Characterization

To analyze the density of the samples, five specimens of dimensions 25 mm × 25 mm × 25 mm were used per sample, and the densities of the foams were calculated using Equation 1, as described in ASTM D3574-11. Each value was calculated as the average of seven independent measurements (seven specimens per formulation).

$$\rho_f = \frac{m_f}{v_f} \times 10^6 \quad (1)$$

where ρ_f , m_f , and v_f represent the foam density (kg.m⁻³), the mass (g), and the volume (mm³) of the specimen, respectively.

The sample morphology was examined via field-emission scanning electron microscopy (FEG-SEM) on a Shimadzu

device (Superscan SS-550 model) and a Tescan microscope (model Mira3). All samples were pre-coated with gold, and a voltage of 15 kV was used. The foam area was observed vertically in the direction of sample expansion.

Three specimens of dimensions approximately 25 mm × 25 mm × 25 mm were conditioned in an environment with a temperature of 23 ± 2 °C and a relative humidity of 60 ± 5% to assess the hydrophobic properties of the coated foam. The samples were then placed under a glass slide, and a drop of deionized water was added to a glass syringe at five different points under the same conditions. Images were taken with a Lumix FZ40 digital camera as soon as the drop touched the surface of the sample and after 5 min, and were analyzed using SurfTens software (version 3.0).

Chemical properties were evaluated using a Nicolet iS10 Fourier-transform infrared (FTIR) spectrometer (Thermo Scientific) with attenuated total reflectance (ATR). The samples were scanned at a resolution of 4 cm⁻¹ in the wavenumber range of 4000–400 cm⁻¹.

The thermal properties of the foams were evaluated using a thermogravimetric analyzer (TGA) (Shimadzu model TGA-50) with a heating ramp of 23–800 °C at a rate of 10 °C.min⁻¹ in a nitrogen atmosphere (50 mL.min⁻¹). Each assay used approximately 10 mg of each sample.

Compressive strength tests on the PU foams were performed using universal testing equipment, EMIC model DL 2000, with specimens of dimensions 50 mm × 50 mm × 25 mm and a compression speed of 50 mm.min⁻¹. The tension required to reduce the thickness of a specimen by up to 80% of its initial thickness was evaluated using ASTM D3574-11. Tests were performed on five specimens.

Static sorption tests were performed using the ASTM F726-12 methodology, in which the sorbent was added to the oil for 15–30 min (sorption time increased with increasing oil viscosity) until the samples were completely submerged in the oil. Following that, the samples were withdrawn,

suspended for 30 s to drain excess oil (desorption), and reweighed. The dimensions of the samples used in the tests were 25 mm × 25 mm × 25 mm. All samples were evaluated in triplicate, and the tests were performed at 23 °C.

To calculate the sorption capacity of the PU foams, two methods were used: (1) the standard method, which evaluates the sorption capacity as a function of the mass of the sorbent before and after the test, as represented in Equation 2, and (2) sample collection capacity. Concerning the collection of oil per sample, the test specimens with a constant volume (25 mm × 25 mm × 25 mm) and exposed to different types of oils according to the previously described methodology were compressed (crushed) for maximum oil removal from the body of the foam. The oil collected from the test specimens (in a constant volume) was then weighed (measured in units) in grams, and all tests were performed in triplicate.

$$SC = \frac{M1 - M0}{M0} \quad (2)$$

where *SC*, *M0*, and *M1* represent the sorption capacity (g.g⁻¹) and the mass (g) of the dry sorbent and the mass (g) of the sorbent added to the sorbate, i.e., the mass after the sorption test, respectively.

3. Results and Discussions

Figure 2 depicts SEM micrographs of PU foams with varying cellulose contents. All samples were predominantly composed of open cells. There were no significant differences in the morphologies of the PU foam cells with different cellulose contents. The MCC was deposited inside the solid phase of the foam (PU) and exhibited no effect on cell nucleation during foam expansion.

Figure 3 depicts the bulk densities of PU foams with different MCC contents and foams samples after organosilane treatment (PU.S). Increasing the MCC content causes an increase in the bulk density of the samples, which is to be expected given that cellulose is an additional component. It is also necessary to consider that the addition of cellulose to polyol causes a proportional increase in the viscosity of this phase, which restricts the expansion capacity of the foam. This is coupled with the fact that cellulose fibers occupy the empty spaces within the PU molecules and can promote an increase in foam density^[23].

It was also discovered that following the hydrophobic chemical treatment, all samples exhibited higher density than their non-chemically treated counterparts, which is associated with the incorporation of organosilane layers on the surface of the solid fraction of the foam. It is noteworthy that, when compared to the pure PU sample (which increased by approximately 7%), the samples containing MCC following chemical treatment increased in density, with increases of 27, 29, 20, and 14% for PU.C10, PU.C20, PU.C30, and PU.C40, respectively. The increase in density of the foams with MCC could be attributed to an increase in the surface roughness of the solid fraction, which could have resulted in the formation of thicker layers of organosilane on the surface of the foam solid fraction.

Figure 4 depicts the FTIR spectra of PU foam (without cellulose) before and after organosilane coating. Only the PU sample spectra are shown in this figure because cellulose was deposited inside the solid fraction rather than on the surface in the PU foam samples with MCC, and no significant difference was observed between the PU samples with and without MCC. A band was observed at 3320 cm⁻¹, corresponding to the N-H group (urethane); a nearby peak at 2272 cm⁻¹, attributed to the NCO group present in the isocyanate; absorption bands at 1224 cm⁻¹ and

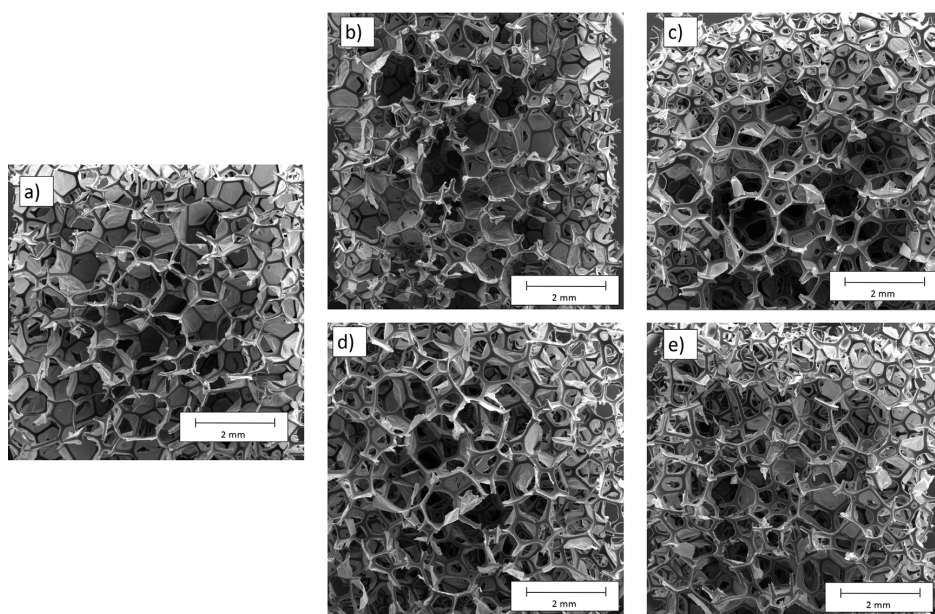


Figure 2. SEM images of the morphology of (a) PU; (b) PU.C10; (c) PU.C20; (d) PU.C30; and (e) PU.C40 foams.

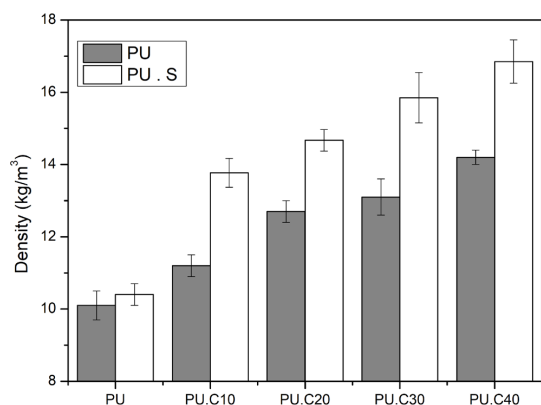


Figure 3. Densities of PU samples with varying MCC contents and without/with organosilane-based hydrophobic treatment.

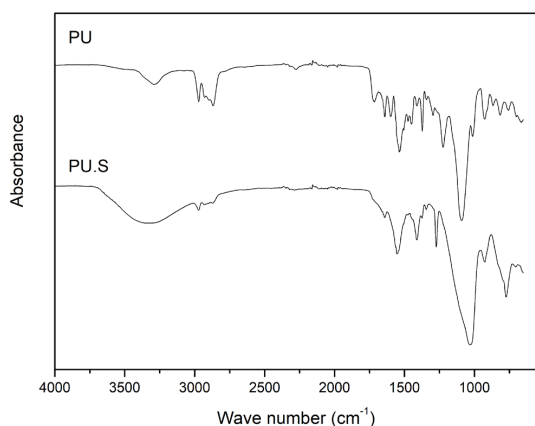


Figure 4. FTIR spectra of PU sample foams (without cellulose), before and after coating with organosilane.

1513 cm^{-1} , arising from the presence of the N–H and N–C groups, respectively; and a peak at 1725 cm^{-1} , attributed to the presence of the carbonyl (C=O) group. The band at 1075–1115 cm^{-1} is assigned to C–O–C groups, the band at 2880–2890 cm^{-1} is assigned to CH groups, and the bands at 1605, 1540, and 870 cm^{-1} are due to aromatic structures, such as C=C of the benzene ring^[24].

The appearance of a band at 765 cm^{-1} that is related to Si–C was observed in the samples treated with the organosilane coating^[25] and an increase in the intensity of the band near 3500 cm^{-1} , which may be due to the presence of OH– terminal groups of the hydrolyzed organosilane. The disappearance of several PU characteristic bands was observed following chemical treatment, which may be due to the test method used (FTIR–ATR spectroscopy), in which the depth of penetration of the beam interferes with the existing bonds in the PU with the hydrophobic coating.

Figure 5 depicts the stress–strain curves of PU foams with various cellulose contents. All samples exhibited the typical deformation behavior of polymeric foam, with three well-defined stages: (I) deformation, (II) plateau, and

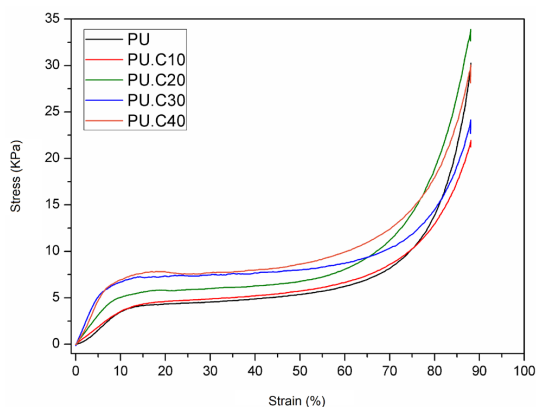


Figure 5. Stress–strain of PU foams with different MCC contents.

(III) densification, as determined by analyzing the curves obtained by compressing the foams with deformations up to 80% of the initial volume^[26]. The first linear stage (elastic) deformation is related to the modulus of elasticity and consists of a reversible deformation responsible for the bending and distension of the cell walls. That is, the cell must be able to withstand the applied force without deforming its geometric shape. After reaching the critical stress value of the elastic region, the cell begins to deform, and in general, the sample exhibits low resistance and mechanical response during this phase. When the deformation reaches its maximum value, the solid fraction of the polymeric matrix is compacted^[27].

Analyzing the PU samples with various MCC contents reveals a tendency for mechanical resistance to increase by compression with an increase in cellulose content in the foams. According to Hussain and Kortschof^[23] short fibers are preferentially deposited inside the polymer matrix in the contours of the cells. Because cellulose exhibits a high concentration of hydroxyl groups in its chemical structure, it is assumed to have a strong interaction with the polyol used in the formulation of PU foams, promoting the strengthening and stiffening effects of the polymer matrix^[23]. The morphology of the cells in the PU foams with different cellulose contents did not change significantly, leading to the conclusion that the stiffening of the polymer matrix combined with the increased density of the foams in the presence of cellulose fibers were the primary factors contributing to the increase in compressive strength of PU foams reinforced with different cellulose contents.

Figure 6 depicts thermogravimetric thermal characterization. The PU experienced two stages of mass loss, as previously described. The second event of the degradation thermogram shows an increase in the degradation temperature with increasing cellulose content. According to Borsoi et al.^[28], the primary degradation event in the thermogravimetry degradation of MCC in an N_2 atmosphere at a rate of 10 $^\circ\text{C}/\text{min}$ occurs in the temperature range of 338–376 $^\circ\text{C}$, which would justify the increase in degradation temperature in this second event with increasing cellulose content in PU foams. Furthermore, cellulose is mixed with polyols in the formulation, which may result in strong interactions between the phases.

Figure 7 depicts SEM micrographs of PU samples with various MCC levels, with and without hydrophobic treatment. It is possible to observe that following the organosilane treatment, the samples exhibited a rigid coating layer that

was fragmented during the cutting process, making the organosilane coating layer more evident. Pure PU exhibits a smoother surface before chemical treatment, which may contribute negatively to the adhesion of the organosilane to the surface; under mechanical effects, it deteriorates and is more easily removed. As observed in the micrographs, the presence of MCC resulted in thicker layers of organosilane and no significant cracks or detachments compared to PU.

The hydrophobicity of the PU foams was determined by measuring the contact angle of their (pressed) surface with water (polar liquid), which is defined as the angle between the solid surface and the tangent line of the liquid phase at the solid phase interface. Figure 8 lists the contact angles of the water droplet and the PU foam surface.

At time $t = 0$, the contact angle obtained for all samples silanized with a liquid with maximum surface tension (water) was greater than 110° , indicating a surface with hydrophobic properties. The water droplet angle above cellulose-reinforced foams increased slightly, probably because of the increased interaction of the foam surface with organosilane.

The contact angle of water with the substrate surface is related to the functional groups present on the solid surface of the PU foam. After 5 min of testing, water

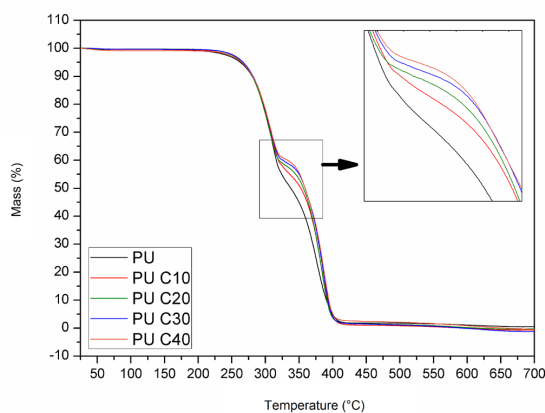


Figure 6. Degradation thermograms of PU foams with different cellulose contents (uncoated).

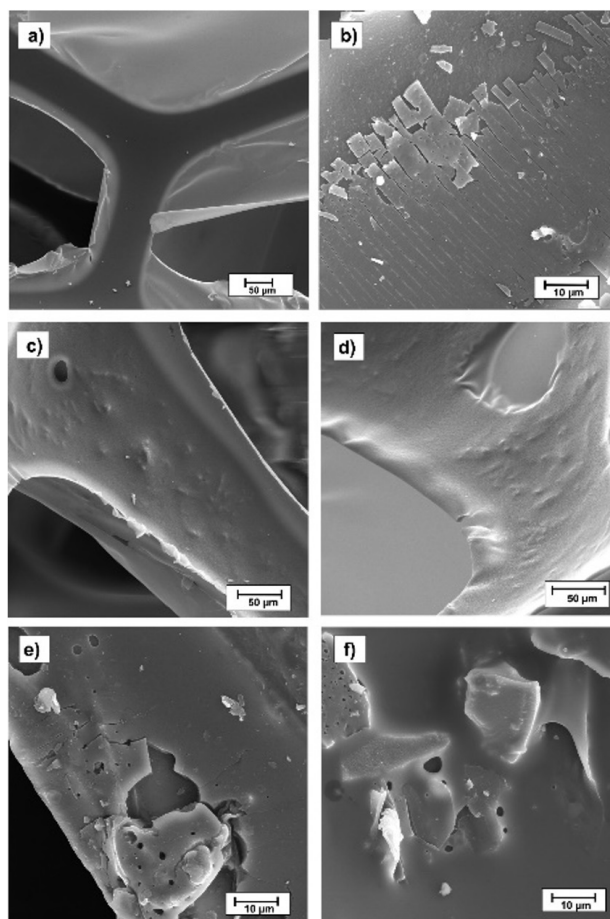


Figure 7. SEM images of (a) untreated pure PU, (b) pure PU with organosilane, (c) and (d) untreated PU.C40, and (e) and (f) PU.C40 with organosilane.

Sample	Angle (t=0 minutes)		Angle (t=5 minutes)	
PU		77.8°		49.5°
PU.S		110.2°		105.7°
PU.C10.S		121.4°		116.4°
PU.C20.S		117.3°		107.2°
PU.C30.S		116.1°		106.3°
PU.C40.S		116.6°		107.1°

Figure 8. Contact angles between the water droplet and the PU foam surface with and without coating and different cellulose contents.

droplet measurements on the silanized PU foam exhibited a slight decrease in contact angle compared to that at $t = 0$, probably owing to water migration into the compensated porous structure^[29]. After 5 min, the foams without chemical treatment showed greater water migration into the foam.

According to the results, all organosilane-treated samples were hydrophobic. According to Cunha et al. (2010)^[30], the hydrophobicity of a material can be evaluated using the contact angle of a drop of water deposited on its surface. When the contact angle is greater than 90° , it is considered hydrophobic. The greater the contact angle, when considering water as the fluid, the greater the hydrophobic selectivity, preventing the foam adsorbing water during exposure to dynamic environments (water and oil)^[29].

Figure 9 depicts the static sorption capacity of PU foams with varying cellulose contents coated with organosilane and the influence of various types of oils. The sorption capacity was associated with oil viscosity and foam density. First, PU foams with more viscous oils exhibited higher sorption capacities. This phenomenon is primarily attributed to oil desorption after its removal from the system. More viscous oils have a more difficult time flowing out of the foam and require longer desorption times; thus, a greater amount of oil is retained inside the foam. Because the desorption time for all samples was set to 30 s, it was expected that the foams would have a higher sorption capacity for more viscous oils. The sorption process is directly influenced by the viscosity of the oil, and oils with high viscosity are more easily anchored and retained in porous polymer systems than oils with less viscosity.

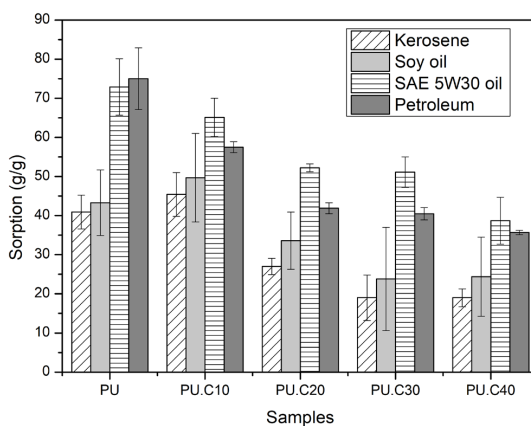


Figure 9. Static sorption capacities of PU foams with different cellulose contents.

A comparative analysis of the samples revealed that as the cellulose content in the PU foams increased, the sorption capacity decreased for all oils. Because the morphologies of the cell structures of the foams were similar, this decrease in sorption capacity was directly associated with an increase in density with increasing cellulose content. Duong and Burford^[8] investigated the effect of the sorption capacity of PU foams by evaluating the effect of the density of PU foams, viscosities of oils, and temperature on the sorption

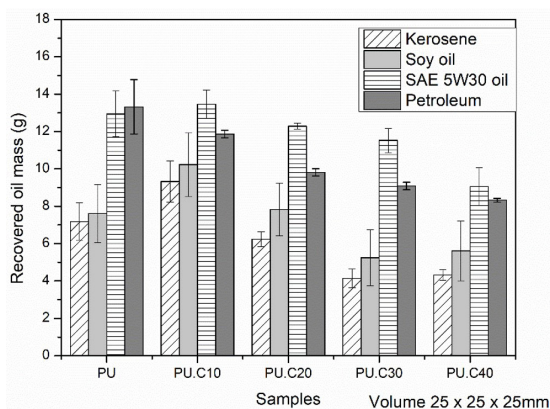


Figure 10. Oil collection, in grams, of PU foams with varying cellulose content and coated with organosilane.

behavior of oils in different PU foams. They reported that the sorption capacity increased significantly with decreasing foam density owing to an increase in the number of open cells and cell morphology, and that this behavior was also affected by oil viscosity and temperature (test temperature).

Figure 10 depicts the sorption capacity in grams of oil per gram of sorbent. Because the increase in sample mass (constant volume) is directly related to the sorption capacity of the foam, as the foam density increases, the sorption capacity tends to decrease. Figure 9 depicts the amount of oil (g) collected per specimen with the same dimensions to evaluate the oil collection capacity per unit volume of sorbent.

According to the data in Figure 10, the recovered oil mass of the samples with each of the oils was observed to be collected by the samples; however, SAE 5W30 oil was the most abundant mass removed, followed by petroleum. As previously stated, sorption capacity is associated with oil viscosity and foam density. Because the morphologies of the foam cell structures were similar, the sorption was directly associated with the increase in density of the foams with increasing cellulose content.

4. Conclusions

PU foams reinforced with MCC chemically modified with organosilane were successfully developed as an absorbent system, as the contact angle test and sorption capacity of the samples could be visualized. Developing a mechanism that satisfies some of the requirements for oil-in-water removal. Although the morphology of the cells in PU foams with different cellulose contents did not change significantly, the MCC content increased compressive strength, which can be attributed to an increase in density combined with stiffening of the polymer matrix. The results of the sorption capacity tests demonstrate that higher-density foams, such as PU foams, have the worst sorption capacity. Therefore, the presence of micro cellulose affected the decrease in oil sorption and collection capacity, which is related to the improvement in material density. Although the use of MCC in the composition is responsible for the higher density, which negatively affects the sorption capacity of the samples, the

presence of cellulose increased the surface roughness of the PU and provided better adhesion and anchoring of the chemical treatment based on organosilane in the foam, as observed during the characterization stage. Nevertheless, the obtained samples exhibited hydrophobic and oleophilic properties. Microcrystalline polymeric foams are an appealing and promising solution for the oil spill environmental problem, especially when compared to conventionally used inorganic fillers, which are relatively low in cost and density.

5. Author's Contribution

- **Conceptualization** – Matheus Vinícius Gregory Zimmermann.
- **Data curation** – Matheus Vinícius Gregory Zimmermann.
- **Formal analysis** – Matheus Vinícius Gregory Zimmermann.
- **Funding acquisition** – Ademir José Zattera; Ruth Marlene Campomanes Santana.
- **Investigation** – Matheus Vinícius Gregory Zimmermann.
- **Methodology** – Matheus Vinícius Gregory Zimmermann.
- **Project administration** – Ademir José Zattera.
- **Resources** – Ademir José Zattera; Ruth Marlene Campomanes Santana.
- **Software** – Marina Kauling de Almeida; Lara Vasconcellos Ponsoni.
- **Supervision** – Ademir José Zattera; Ruth Marlene Campomanes Santana.
- **Validation** – Marina Kauling de Almeida; Lara Vasconcellos Ponsoni.
- **Visualization** – Eduardo Junca; Marina Kauling de Almeida; Lara Vasconcellos Ponsoni; Tiago Mari.
- **Writing – original draft** – Matheus Vinícius Gregory Zimmermann; Marina Kauling de Almeida; Lara Vasconcellos Ponsoni.
- **Writing – review & editing** – Eduardo Junca; Tiago Mari.

6. Acknowledgements

Funding: This study was supported by the National Council for Scientific and Technological Development (CNPq).

7. References

1. ITOPE. (2023). *Oil tanker spill statistics 2022*. Retrieved in 2023, April 25, from <https://www.itopf.org/knowledge-resources/data-statistics/statistics/>
2. Wan, Z., & Chen, J. (2018). Human errors are behind most oil-tanker spills. *Nature*, 560(7717), 161-163. <http://dx.doi.org/10.1038/d41586-018-05852-0>. PMID:30082696.
3. Zhang, M., Su, M., Qin, Y., Liu, C., Shen, C., Ma, J., & Liu, X. (2023). Photothermal ultra-high molecular weight polyethylene/MXene aerogel for crude oil adsorption and water evaporation. *2D Materials*, 10(2), 024007. <http://dx.doi.org/10.1088/2053-1583/acc3aa>.
4. Ivshina, I. B., Kuyukina, M. S., Krivoruchko, A. V., Elkin, A. A., Makarov, S. O., Cunningham, C. J., Peskur, T. A., Atlas, R.

- M., & Philip, J. C. (2015). Oil spill problems and sustainable response strategies through new technologies. *Environmental Science. Processes & Impacts*, 17(7), 1201-1219. <http://dx.doi.org/10.1039/C5EM00070J>. PMID:26089295.
5. Lim, T.-T., & Huang, X. (2007). Evaluation of kapok (Ceiba pentandra (L.) Gaertn.) as a natural hollow hydrophobic-oleophilic fibrous sorbent for oil spill cleanup. *Chemosphere*, 66(5), 955-963. <http://dx.doi.org/10.1016/j.chemosphere.2006.05.062>. PMID:16839589.
 6. Centro de Recursos Ambientais – CRA. (2002). *Ecotoxicologia e avaliação de risco do petróleo*. Salvador: CRA. Retrieved in 2023, April 25, from <http://www.w2s3.com.br/download/Ecotoxicologia%20e%20Avaliacao%20de%20Risco%20do%20Petroleo.pdf>
 7. Zimmermann, M. V. G., Zattera, A. J., Fenner, B. R., & Santana, R. M. C. (2021). Sorbent system based on organosilane-coated polyurethane foam for oil spill clean up. *Polymer Bulletin*, 78(3), 1423-1440. <http://dx.doi.org/10.1007/s00289-020-03169-5>.
 8. Duong, H. T. T., & Burford, R. P. (2006). Effect of foam density, oil viscosity, and temperature on oil sorption behavior of polyurethane. *Journal of Applied Polymer Science*, 99(1), 360-367. <http://dx.doi.org/10.1002/app.22426>.
 9. Liu, Y., Ma, J., Wu, T., Wang, X., Huang, G., Liu, Y., Qiu, H., Li, Y., Wang, W., & Gao, J. (2013). Cost-effective reduced graphene oxide-coated polyurethane sponge as a highly efficient and reusable oil-absorbent. *ACS Applied Materials & Interfaces*, 5(20), 10018-10026. <http://dx.doi.org/10.1021/am4024252>. PMID:24050505.
 10. Bayat, A., Aghamiri, S. F., Moheb, A., & Vakili-Nezhaad, G. R. (2005). Oil spill cleanup from sea water by sorbent materials. *Chemical Engineering & Technology*, 28(12), 1525-1528. <http://dx.doi.org/10.1002/ceat.200407083>.
 11. Chung, S., Suidan, M. T., & Venosa, A. D. (2011). Partially Acetylated Sugarcane Bagasse for Wicking Oil from Contaminated Wetlands. *Chemical Engineering & Technology*, 34(12), 1989-1996. <http://dx.doi.org/10.1002/ceat.201100353>.
 12. Andersons, J., Kirpluks, M., & Cabulis, U. (2020). Reinforcement efficiency of cellulose microfibrils for the tensile stiffness and strength of rigid low-density polyurethane foams. *Materials (Basel)*, 13(12), 2725. <http://dx.doi.org/10.3390/ma13122725>. PMID:32549317.
 13. Jianliang, X., Nana, L., Xinfeng, X., Yu, B., Yu, G., Kunhua, W., Xiangming, H., Dongle, C., & Qing, J. (2022). Durable hydrophobic Enteromorpha design for controlling oil spills in marine environment prepared by organosilane modification for efficient oil-water separation. *Journal of Hazardous Materials*, 421, 126824. <http://dx.doi.org/10.1016/j.jhazmat.2021.126824>. PMID:34396973.
 14. Usman, J., Othman, M., Ismail, A. F., Rahman, M. A., Jaafar, J., Raji, Y. O., El Badawy, T. H., Gbadamosi, A. O., & Kurniawan, T. A. (2020). Impact of organosilanes modified superhydrophobic-superoleophilic kaolin ceramic membrane on efficiency of oil recovery from produced water. *Journal of Chemical Technology and Biotechnology (Oxford, Oxfordshire)*, 95(12), 3300-3315. <http://dx.doi.org/10.1002/jctb.6554>.
 15. Salon, M.-C. B., Abdelmouleh, M., Boufi, S., Belgacem, M. N., & Gandini, A. (2005). Silane adsorption onto cellulose fibers: hydrolysis and condensation reactions. *Journal of Colloid and Interface Science*, 289(1), 249-261. <http://dx.doi.org/10.1016/j.jcis.2005.03.070>. PMID:15907861.
 16. Abdelmouleh, M., Boufi, S., Ben Salah, A., Belgacem, M. N., & Gandini, A. (2002). Interaction of silane coupling agents with cellulose. *Langmuir*, 18(8), 3203-3208. <http://dx.doi.org/10.1021/la011657g>.
 17. Shan, C. W., Idris, M. I., & Ghazali, M. I. (2012). Study of flexible polyurethane foams reinforced with coir fibres and tyre particles. *International Journal of Applied Physics and Mathematics*, 2(2), 123-123. <http://dx.doi.org/10.7763/IJAPM.2012.V2.67>.
 18. Zimmermann, M. V. G., Turella, T., Santana, R. M. C., & Zattera, A. J. (2014). Comparative study between poly(ethylene-co-vinyl acetate) – EVA expanded composites filled with banana fiber and wood flour. *Materials Research*, 17(6), 1535-1544. <http://dx.doi.org/10.1590/1516-1439.269814>.
 19. Jonoobi, M., Harun, J., Mathew, A. P., Hussein, M. Z. B., & Oksman, K. (2010). Preparation of cellulose nanofibers with hydrophobic surface characteristics. *Cellulose (London, England)*, 17(2), 299-307. <http://dx.doi.org/10.1007/s10570-009-9387-9>.
 20. Goussé, C., Chanzy, H., Cerrada, M. L., & Fleury, E. (2004). Surface silylation of cellulose microfibrils: preparation and rheological properties. *Polymer*, 45(5), 1569-1575. <http://dx.doi.org/10.1016/j.polymer.2003.12.028>.
 21. Kuboki, T., Lee, Y. H., Park, C. B., & Sain, M. (2009). Mechanical properties and foaming behavior of cellulose fiber reinforced high-density polyethylene composites. *Polymer Engineering and Science*, 49(11), 2179-2188. <http://dx.doi.org/10.1002/pen.21464>.
 22. Trache, D., Hussin, M. H., Chuin, C. T. H., Sabar, S., Fazita, M. R. N., Taiwo, O. F. A., Hassan, T. M., & Haafiz, M. K. (2016). Microcrystalline cellulose: isolation, characterization and bio-composites application – A review. *International Journal of Biological Macromolecules*, 93(Pt A), 789-804. <http://dx.doi.org/10.1016/j.ijbiomac.2016.09.056>.
 23. Hussain, S., & Kortschot, M. T. (2015). Polyurethane foam mechanical reinforced by low-aspect ratio micro-crystalline cellulose and glass fibres. *Journal of Cellular Plastics*, 51(1), 59-73. <http://dx.doi.org/10.1177/0021955X14529137>.
 24. Li, H., Liu, L., & Yang, F. (2012). Hydrophobic modification of polyurethane foam for oil spill cleanup. *Marine Pollution Bulletin*, 64(8), 1648-1653. <http://dx.doi.org/10.1016/j.marpolbul.2012.05.039>. PMID:22749062.
 25. Gwon, J. G., Lee, S. Y., Chun, S. J., Doh, G. H., & Kim, J. H. (2010). Effects of chemical treatments of hybrid fillers on the physical and thermal properties of wood plastic composite. *Composites. Part A, Applied Science and Manufacturing*, 41(10), 1491-1497. <http://dx.doi.org/10.1016/j.compositesa.2010.06.011>.
 26. Saha, M. C., Mahfuz, H., Chakravarty, U. K., Uddin, M., Kabir, M. E., & Jeelani, S. (2005). Effect of density, microstructure, and strain rate on compression behavior of polymeric foams. *Materials Science and Engineering A*, 406(1-2), 328-336. <http://dx.doi.org/10.1016/j.msea.2005.07.006>.
 27. Gibson, L. J., & Ashby, M. F. (1997). *Cellular solids: structure and properties*. USA: Cambridge University Press. <http://dx.doi.org/10.1017/CBO9781139878326>.
 28. Borsoi, C., Zimmermann, M. V. G., Zattera, A. J., Santana, R. M. C., & Ferreira, C. A. (2016). Thermal degradation behavior of cellulose nanofibers and nanowhiskers. *Journal of Thermal Analysis and Calorimetry*, 126(3), 1867-1878. <http://dx.doi.org/10.1007/s10973-016-5653-x>.
 29. Wu, Z.-Y., Li, C., Liang, H.-W., Chen, J.-F., & Yu, S.-H. (2013). Ultralight, flexible, and fire-resistant carbon nanofiber aerogels from bacterial cellulose. *Angewandte Chemie International Edition in English*, 52(10), 2925-2929. <http://dx.doi.org/10.1002/anie.201209676>. PMID:23401382.
 30. Cunha, A. G., Freire, C., Silvestre, A., Pascoal, C., No., Gandini, A., Belgacem, M. N., Chaussy, D., & Beneventi, D. (2010). Highly hydrophobic biopolymers prepared by the surface pentafluorobenzoylation of cellulose substrates. *Journal of Colloid and Interface Science*, 344(2), 588-595. <http://dx.doi.org/10.1016/j.jcis.2009.12.057>. PMID:20129622.

Received: Aug. 02, 2023

Revised: Sept. 19, 2023

Accepted: Oct. 10, 2023